Rapid Evaporative Cooling Suppresses Fragmentation in Mass Spectrometry: Synthesis of "Unprotonated" Water Cluster Ions

Rienk T. Jongma, Yuhui Huang, Shiming Shi, and Alec M. Wodtke*

Department of Chemistry, University of California, Santa Barbara, California 93106

Received: August 13, 1998; In Final Form: September 2, 1998

Hydrogen-bonded water clusters were formed with inert gases adsorbed to them in a strong molecular beam expansion. Upon single-photon ionization of such mixed clusters using VUV light, fragmentation of the substrate water cluster ion is markedly suppressed. Experimental evidence is presented, showing that the rapid evaporation of the inert gas from the newly formed water cluster ion efficiently removes internal energy on a time scale much faster than the usual fragmentation reactions present in pure water clusters, i.e., rates of fragmentation that are normally $>10^9$ s^{-1}. This phenomenon is exploited to produce "unprotonated" water clusters, formally $(H_2O)_n^+$. Using post source decay reflectron time-of-flight mass spectrometry, the structure of the "unprotonated" water cluster ions is experimentally determined for the first time. The structure determined, $H_3O^+(H_2O)_k$·OH where the hydroxyl radical is found outside the first solvation shell of the charge, is consistent with recent ab initio calculations. This simple approach to the control of fragmentation in mass spectrometry appears to have promise in applications to other interesting polymeric samples, for example biopolymers.

Introduction

The existence of "unprotonated" water cluster ions, nominally $(H_2O)_n^+$, has been known since the observation of the water dimer ion[1] and has been more recently reported for larger clusters sizes.[2,3] Experimental determination of the structure and chemical properties of these ions has been hampered by our inability to suppress fragmentation resulting from the ionization process. Vertical ionization of water clusters initially forms a solvated H_2O^+ ion in a fragile "polymeric molecule" far removed from its lowest energy structure. As a consequence, a rapid intracluster proton-transfer reaction results: $H_2O^+ + H_2O \rightarrow H_3O^+ + OH$, releasing about 1 eV of energy.[4] The orientation of the solvent water molecules also exhibits slower but still rapid reorganization to accommodate the newly formed charge. This so-called solvation energy deposits an additional 1−2 eV of internal energy into the cluster.[5,6]

The binding energy of the cluster constituents is measured in tenths of electronvolts. Consequently, fragmentation of the parent cluster ion is expected and observed. Loss of the newly formed OH, which is the most weakly bound component of the cluster, occurs on a subnanosecond time scale for clusters containing less than ∼70 water molecules.[7] This means that a family of neutral water clusters, $(H_2O)_{n+1}$ ($n \geq 1$), is observed as a series of mass features no heavier than, H_3O^+ $(H_2O)_{n-1}$ (alternatively written as $(H_2O)_nH^+$). In this work such clusters will be designated as p^n, that is, protonated water clusters with "n" solvent water molecules. The subsequent evaporation of water monomers from the protonated ion ($p^n \rightarrow p^{n-m} + mH_2O$) can also easily be observed, for example, in a reflectron time-of flight (TOF) mass spectrometer.[8]

There are two logical possibilities to suppress fragmentation resulting from ionization. One may seek means of ionization that deposit little or no energy into the parent ion (soft ionization), or one may attempt to remove the energy that is deposited into the parent ion (active parent ion cooling). Up to now, nearly all attempts to suppress fragmentation have been various forms of soft ionization. For example, in photoionization, tuning the wavelength close to the adiabatic ionization potential is one way to lower the amount of energy deposited into the parent ion. However, when the ion structure and the neutral structure are substantially different, the ionization cross section is usually bound by the Franck−Condon principle to be vanishingly small near the adiabatic threshold. As a practical matter, then, it may be necessary to ionize well above the adiabatic threshold to obtain sufficient ionization efficiency.

There is some evidence that ion fragmentation of guest molecules in host van der Waals clusters is reduced. In one work, large superfluid He clusters were formed in molecular beams with stagnation pressures of 20−80 bar and nozzle temperatures of 4−30 K. When SF_6 monomers and dimers were adsorbed on and dissolved in these clusters using the pickup technique,[9] electron impact ionization resulted in reduced parent-ion fragmentation.[10] Although similar experiments on solid Ne clusters did not show this effect,[10] electron bombardment ionization of $(CH_3OH)_n$ and $(CH_3F)_n$ ($n = 1-3$) deposited on large Ar clusters did exhibit suppressed fragmentation.[11] For a number of organic molecules complexed with H_2O and CH_3OH, electron impact ionization of van der Waals molecules formed in a supersonic molecular beam (termed cluster chemical ionization) also exhibited reduced parent ion fragmentation.[12] All of these studies suggest that clusters may be exploited to alter the dynamics of ion fragmentation. However, the mechanisms of cluster-induced suppressed fragmentation have not been experimentally clarified.

In this work we demonstrate a remarkably simple approach to suppress fragmentation in mass spectrometry of large fragile species by active cooling of the newly formed parent ion. For the first time, a systematic investigation of the fragmentation of pure and mixed water clusters explicitly reveals the mechanism responsible for the active cooling observed for mixed (rare gas containing) clusters. We have obtained clear evidence

10.1021/jp983366v CCC: $15.00
Published on Web 10/14/1998

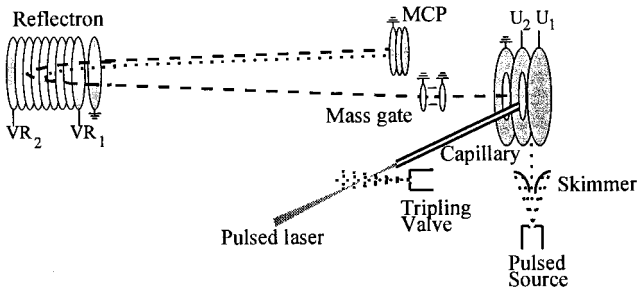

Figure 1. Schematic representation of the reflectron TOF mass spectrometer. A pulsed source expands a mixture of water and carrier gas into the source chamber. After the molecular beam is skimmed, it enters the ion source of the mass spectrometer. Neutral water clusters are ionized using XUV radiation, produced by frequency tripling the second harmonic of a pulsed dye laser in a pulsed jet. The XUV light thus obtained is captured by a quartz capillary and guided to the ion source. The water cluster ions are extracted by the applied electric fields into the drift tube. A mass gate mounted in this tube can select part of the spectrum. Parent and daughter ions are separated in time in the reflectron (respective trajectories indicated by the dashed and by the dotted line) and are detected on a MCP detector after passing the second field-free region.

for rapid cooling of parent water cluster ions by evaporation of preadsorbed carrier gas. In high-pressure molecular beam expansions, the analyte may be "coated with carrier gas", forming mixed neutral clusters $(H_2O)_pM_q$ where we have used M = Ar, Kr, N_2, CO, CO_2, and O_2. Single-photon ionization of the mixed water clusters, well above the adiabatic ionization potential, is followed by rapid loss of carrier gas resulting in evaporative cooling, strongly suppressing all fragmentation pathways. We have exploited this technique to synthesize a series of "unprotonated" water cluster ions with the nominal chemical formula $(H_2O)_n^+$. We have analyzed the metastable decay of these ions in a reflectron TOF mass spectrometer to show that their structure is best described as $H_3O^+(H_2O)_{n-2}\cdot OH$, where intracluster proton transfer is followed by diffusion of the OH product out of the first solvation shell.

Experimental Setup

A schematic overview of the molecular beam photoionization reflectron[13] TOF mass spectrometer used in these experiments is shown in Figure 1. A mixture of room-temperature water vapor and carrier gas (total backing pressure between 2 and 6 bar) is expanded through a pulsed (200 μs duration) solenoid valve (General Valve). The standard orifice of the valve is replaced with a slowly diverging conical nozzle (smallest diameter: 0.8 mm) to enhance water cluster formation. The gas mixture is expanded into the source chamber (pumped by an 1100 L/s turbomolecular pump). Under these conditions the cooling during the expansion allows efficient production of clusters containing up to ~80 water monomers. After passing a 0.5 mm diameter skimmer, the molecular beam enters the ionization region (pumped by a 400 L/s turbomolecular pump) of a reflectron TOF mass spectrometer (R.M. Jordan Co.).

Single-photon ionization of the water clusters is performed with vacuum-ultraviolet (VUV) radiation produced as follows: the output of a Nd:YAG laser (Continuum, PL7010) pumped dye laser (Spectra Physics, PDL-1) running on Fluorescein 548 is frequency doubled in a KDP crystal, providing radiation around 277 nm with an energy of ~15 mJ/pulse in a 0.7 cm^{-1} bandwidth. The second harmonic is separated from the fundamental of the dye laser and guided into a tripling chamber. The laser is focused close to the orifice of a pulsed beam of pure N_2 (General Valve, backing pressure 10 bar) by a lens with a 25 cm focal length. This results in frequency tripling of the 277 nm radiation, which is enhanced by tuning the laser to a well-known two-photon resonance in molecular nitrogen.[14] The VUV radiation (92.5 nm/13.4 eV) is captured by a 37.5 cm long quartz capillary with an inner diameter of 2 mm that guides the VUV radiation (and a large fraction of the remaining 277 nm radiation) to the ion source of the mass spectrometer.[15] A slotted hole is placed about halfway down the capillary so that most of the tripling gas can be pumped out of the capillary into a differentially pumped (70 L/s turbomolecular pump) bridging chamber, thus reducing the gas load of the tripling chamber to the ion source of the mass spectrometer. The capillary provides efficient transfer of the VUV light to the ionization region as well as a $>10^6$ pressure reduction between the tripling chamber and the ionization region. Thus, under typical operating conditions, the tripling chamber exhibits a pressure of $\sim 10^{-2}$ Torr (pumped by a 400 L/s turbo drag pump) while the ionization chamber exhibits a pressure of less than 10^{-8} Torr.

The water clusters are ionized between the first two extraction plates (10 mm apart) of the double electric field ion source[16] of the mass spectrometer and are deflected into the drift tube. The distance from the ion source to the first grid of the reflectron is 1.1 m. The distance from this same grid to the detector, defining the second field-free region, is approximately 0.6 m. A mass gate is mounted in the first field-free region. A voltage difference of 400 V is applied between the plates of the mass gate, rejecting (i.e., deflecting) the majority of the masses. Only a narrow part of the spectrum is transmitted when the applied voltage is pulsed to ground during a certain time interval. Unless stated otherwise, this mass gate is not used (i.e., grounded). Different masses are detected according to their arrival time on a double-staged 40 mm diameter microchannel plate (MCP) detector.

The ion signal detected by the MCP detector is fed into a digitizing oscilloscope with a 10 bit vertical resolution and a 100 MHz sampling rate (LeCroy 9430). The signal is summed over a couple of thousands of laser shots in the 16 bit memory of the oscilloscope and subsequently read out by a PC via a GPIB interface. Triggering of the laser, tripling valve, pulsed source, and oscilloscope is regulated by a delay generator (Stanford Research Systems, DG535).

Results and Discussion

Observation and Structure of "Unprotonated" H_2O Clusters. Analysis of reflectron TOF mass spectra has been described in detail in the literature.[17] As long as the fragmentation time is comparable to the acceleration time in the ion source or longer, the reflectron may be used as an energy analyzer to distinguish parent ions from daughters. As a result of the fact that the recoil energy of daughter ions is usually negligible compared to ion velocities in the mass spectrometer, daughter ions formed in the field-free region between the ion source and the reflectron (post source decay, PSD) are formed with the same velocity as their parents but with reduced mass and therefore reduced kinetic energy. The ratio of the parent to daughter kinetic energy is precisely the ratio of their masses. As shown by the trajectories in Figure 1 (parent, dashed; daughter, dotted), parents always appear at later arrival times (longer trajectories) than do their daughters. By recording the reflectron voltages at which daughters and parents have the same flight time, unambiguous assignments of daughters to parents can be made. Lowering the voltages on the reflectron can also be used to reflect daughters only, as parents will pass through the reflector.

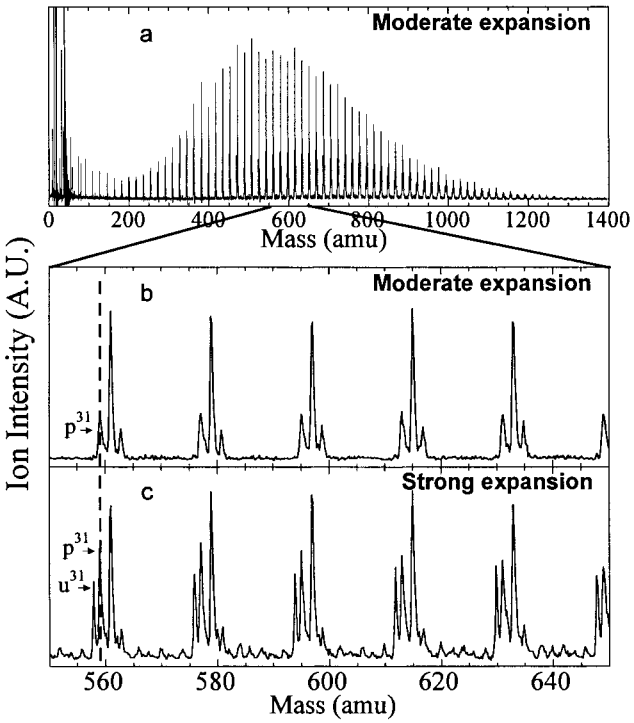

Figure 2. (a) Mass spectrum as recorded using a weak H_2O/Ar expansion. (b) Small part of the same spectrum as displayed in (a), starting at the p^{31}. A progression of "triplets" separated by 18 amu is clearly seen. The first peak of each group is the parent p^n ion for $n = 31-36$. The second and third peaks are daughter ion peaks, produced by loss of one and two water monomers from the protonated parent ion, respectively. (c) Mass spectrum recorded under strong expansion conditions. An extra peak with a mass that is 1 amu less than that of the p^n parent is observed. For comparison, a vertical dashed line indicates the position of the p^{31}. The low mass member of each quartet is assigned as the "unprotonated" water cluster. The structure of these ions is best described as a solvated H_3O^+ ion with an OH radical caged somewhere in the cluster, i.e., $H_3O^+(H_2O)_k$·OH ($k = 29-34$). See text. The small peaks between the quartets are the same unprotonated ions with varying numbers of Ar atoms attached to them.

Figure 2a shows a typical mass spectrum as recorded under modest expansion conditions using Ar as a carrier gas (backing pressure: 2 bar). A long progression of mass features, up to ~1350 amu, resulting from neutral clusters containing up to about 75 water molecules, is readily observed. A small part of this same spectrum (greatly expanded) is shown in Figure 2b. The spectrum appears as a series of "triplets". The protonated parent ion p^{31} (i.e., $H^+(H_2O)_{31}$ produced by intracluster proton transfer and subsequent loss of the OH) is labeled. The low-mass members of each triplet are the p^n ions ($n = 31-36$). The most intense member of each triplet corresponds to protonated ions that have evaporated one water molecule during PSD ($p^n \rightarrow p^{n-1} + H_2O$, where $n = 32-36$). The high-mass member of each triplet corresponds to evaporation of two water molecules during PSD ($p^n \rightarrow p^{n-2} + 2H_2O$, where $n = 33-37$). The rate constant for loss of each additional water monomer decreases rapidly as, for larger water clusters, each evaporated water molecule removes between 0.27 and 0.44 eV from the cluster.[8,18] The low pressure in the field-free drift tube (under these conditions below 3×10^{-8} Torr) almost certainly excludes collisions of cluster ions with background gas, and the observed metastable decay is due to unimolecular decomposition of the energized water cluster ions.

Figure 2b also shows evidence of water evaporation during the time where the ion is accelerated in the ion source, referred to as "in source decay" (ISD). In source decay (ISD) appears as an asymmetric peak shape with a tail to longer flight times (higher masses when converted to the mass scale). The tail terminates on the metastable peak to which it correlates in PSD.[19] Such asymmetric peak shapes are clearly evident for the p^n family of mass features. Although observable, ISD is only a minor contribution to the total metastable decay.

It should be noted that the mass scale that is indicated on the horizontal axis is only valid for the parent ions. Their flight times are proportional to $\sqrt{m}$. Because the mass of the daughter ions changes in the drift tube, this relation is no longer valid, and the horizontal scale is not correct for them. The time delay between parent and daughter ions, however, can be exactly calculated since both geometry of and voltages applied to the reflectron are known.

When backing pressure and driving voltage of the pulsed source are increased (thereby increasing the intensity of the gas pulse), additional families of features are observed in the mass spectrum (Figure 2c). Unlike Figure 2b, this mass spectrum is composed of a series of strong quartets with additional weak mass features between the quartets. The low-mass members of the quartets appear 1 amu lower than the p^n family. (For comparison, a vertical dashed line is indicated in Figure 2b,c.) This family of mass features nominally has the formula $(H_2O)_n^+$ and is formally designated u^n ("unprotonated" cluster ions with n H_2O molecules).

It is extremely unlikely that the proton-transfer reaction between H_2O^+ and H_2O can be suppressed in these clusters, and the formal designation as unprotonated water cluster ions is to be taken as nothing more than nomenclature. Indeed, one must conclude (see below) that the u^n family of mass features results from H_3O^+ $(H_2O)_{n-2}$·OH. To prove this, it was necessary to carry out experiments with beams of D_2O.

In principle, analysis of the PSD of the u^n family could give structural information about these ions. If, as suggested, u^n is due to $H_3O^+(H_2O)_{n-2}$·OH, one might expect to observe loss of OH in the PSD spectrum. Unfortunately, the PSD channels $u^n \rightarrow p^{n-1} + OH$ and $p^n \rightarrow p^{n-1} + H_2O$ appear within 10 ns of one another everywhere in the mass spectrum and cannot be resolved with our apparatus. However, we have found that using beams of heavy water (behaving very similar to the light water cluster beam under all conditions), we can accomplish the unambiguous analysis of the PSD of the u^n family. Figure 3a shows a small part of the TOF spectrum around the arrival time of u^{10} and p^{10} using a strong D_2O/Ar expansion (solid line). The double peak at 37.42 μs is clearly due to two processes (assigned as $u^{11} \rightarrow p^{10} + OD$ and $p^{11} \rightarrow p^{10} + D_2O$). For comparison, one may change the timing between the VUV light pulse and the molecular beam pulse and obtain conditions where no unprotonated cluster ions are formed (dotted line, intensities scaled to p^{10}). Under these conditions only the $p^{11} \rightarrow p^{10} + D_2O$ channel is possible. This confirms that the double peak at 37.42 μs contains (almost equal) contributions of ion signal due to $u^{11} \rightarrow p^{10} + OD$ and ion signal due to $p^{11} \rightarrow p^{10} + D_2O$. The observation of OD loss from u^{11} is unambiguous evidence that the structure of u^{11} is indeed D_3O^+ $(D_2O)_{n-1}$·OD.

Figure 3b gives even clearer evidence of this conclusion. Here a part of the TOF spectrum is shown around the arrival time of u^{20} and p^{20} (solid trace). The dotted trace shows the identical time region for beam conditions that do not produce the u^n family. The PSD channel $p^{21} \rightarrow p^{20} + D_2O$ is hardly detectable for these large clusters and reflects also the anomalous stability of the p^{21} ion (see below). However, the solid trace clearly shows $u^{21} \rightarrow p^{20} + OD$. The 20 ns difference between the two peaks is clearly visible in Figure 3b. The same time

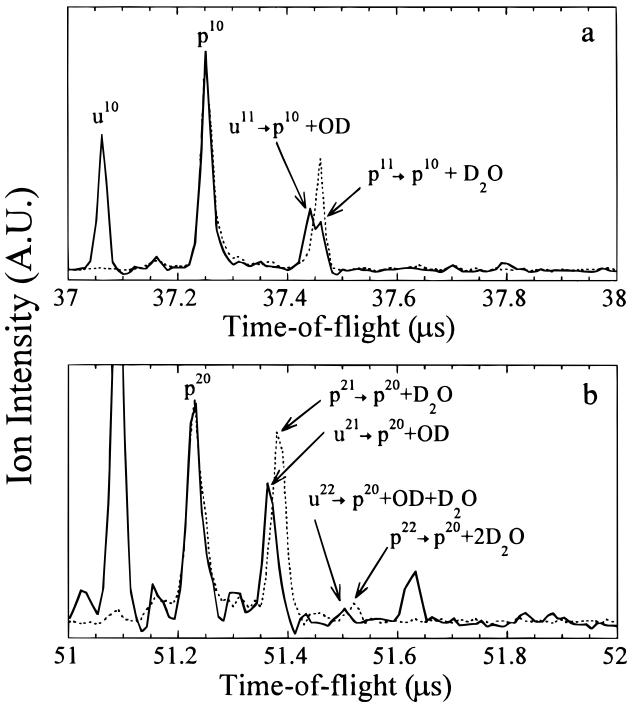

Figure 3. (a) Small part of the TOF spectrum obtained using a D_2O/N_2 expansion. Spectra with (solid line) and without (dashed line) unprotonated cluster signal present are superimposed and scaled to the intensity of the p^{10} peak. The double peak at 37.45 μs (solid line) is due to loss of OD from the unprotonated cluster ($u^{11} \rightarrow p^{10} + OD$) and due to loss of D_2O from the protonated cluster ($p^{11} \rightarrow p^{10} + D_2O$). This assignment is confirmed by the dotted spectrum, where only $p^{11} \rightarrow p^{10} + D_2O$ is possible. (b) Similar to (a) for larger clusters. The presence of the peak due to loss of D_2O from the protonated cluster is hardly detectable under conditions where the unprotonated species is present. The small peak right of this (solid line) is due to the daughter ion produced by loss of OD followed by loss of D_2O from the unprotonated cluster. The peak position of daughter ions due to loss of two D_2O monomers from protonated clusters is at a slightly different position, as is obvious from the dashed spectrum, and is not observed in spectra where the unprotonated clusters appear (solid line).

difference is also visible for the small but detectable peaks due to $u^{22} \rightarrow p^{19} + OD + D_2O$ (solid line) and $p^{22} \rightarrow p^{20} + 2D_2O$.

The observation of OD loss in PSD demonstrates that, under the strong expansion conditions where the u^n family is produced, loss of OD occurs on the tens of microseconds time scale, i.e., the time needed to reach the first reflector grid. The rate of OD loss (normally occurring on a subnanosecond time scale) has been reduced by at least 4 orders of magnitude.

Further analysis of the PSD of the heavy water cluster ions reveals that OD loss from u^n is much more probable than D_2O loss and that D_2O loss never occurs in the absence of OD loss. This observation is not consistent with a hypothetical cluster structure $D_3O^+ \cdot OD\ (D_2O)_{n-2}$, where the OD is always found in the first solvation shell. In that case, OD would be one of the strongest bound constituents of the cluster, and D_2O evaporation (for example, from the second solvation shell) would compete well with OD loss. The fact that OD loss dominates the metastable decay is consistent with an OD molecule that has been formed in the proton-transfer reaction and that has diffused away from the charge center of the cluster. This picture supports findings of recent calculations which show that the OH fragment is loosely bound in unprotonated water clusters at their equilibrium structure.[6]

Figure 4 presents the complete analysis of the PSD of the unprotonated water clusters in terms of relative abundance of

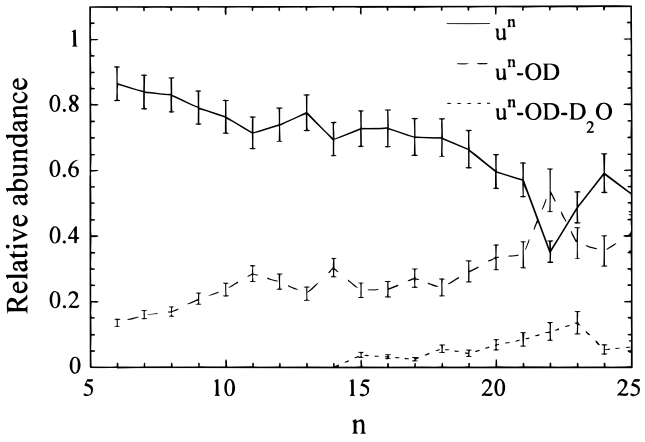

Figure 4. Relative abundance of unprotonated parent ions (solid line) and daughter ions produced by loss of OD from these parents (long-dashed line) or by loss of OD followed by loss of D_2O from the same parents (short-dashed line). The horizontal axis is refers to the cluster size of the parent ion.

parent ions and daughter ions. For the analysis, all double peaks (similar to that in Figure 3a) have been fit to two Gaussians (both having the same width). The double peaks are reproduced very well by the two Gaussians, and the intensity ratio of the two peaks is obtained as a function of cluster size. The ratio between the integrated areas of these two Gaussians is then used to calculate the integrated intensity of the peaks caused by the two different processes, thus allowing quantitative analysis of the PSD of the u^n family. Measurement of the respective decay fractions, as presented in Figure 4, is most accurate when mass spectra are compared where parent and daughter ions follow exactly the same trajectories through the reflector.[17] In this experiment, the parent and daughter ions have different trajectories through the reflector; therefore, a maximum error of 20−30% is expected in the measured integrated intensities for the smallest clusters. This systematic error is however much reduced for the larger clusters observed in this work (and not corrected for because of the large amount of daughter ion peaks for each mass spectrum). In Figure 4 one can see that the fraction of OD loss slowly increases with cluster size. The more efficient production of the "magic" p^{21} (see refs 20−22 and references therein) is also observed as an increase of metastable decay (decrease of u^{22} survival probability, solid line) for u^{22} ($\rightarrow p^{21} + OD$, long-dashed line) and u^{23} ($\rightarrow p^{21} + OD + D_2O$, small-dashed line).

Considering the strong similarities between heavy and light water clusters, we conclude that the structure of the u^n family is $H_3O^+ (H_2O)_{n-2} \cdot OH$. This strongly suggests that this family of mass features originates from neutral water clusters that have undergone the "normal" intracluster proton-transfer reaction and solvent reorganization. The structure also implies that the OH is most frequently not found in the first solvation shell but has begun to diffuse away from the charge center. Empirically, the rate of ion fragmentation (loss of OD) is at least 10 000 times slower under the strong expansion conditions needed to produce the u^n family, consistent with a cluster ion that has undergone substantial cooling of its internal degrees of freedom.

Mechanism for Suppression of Fragmentation. The mechanism for suppression of fragmentation is clearly related to the ionization dynamics of mixed clusters. Referring back to Figure 2c, whenever the beam conditions are adjusted to produce the u^n family of ions, small mass peaks between the main quartets are also always observed, which are due to $H_3O^+(H_2O)_{n-2} \cdot OH\ Ar_m$, i.e., $u^n Ar_m$. In other words, the unprotonated ions can

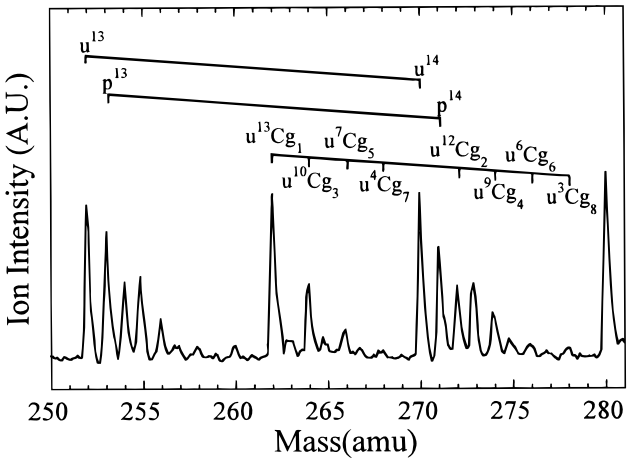

Figure 5. Mass spectrum recorded for a strong H_2O/CO expansion. In addition to the protonated, unprotonated, and daughter ion peaks, strong peaks due to binary H_2O/carrier gas clusters (labeled u^nCg_m, consisting of the unprotonated *n*-mer with *m* carrier gas particles, in this case CO), as assigned in the figure, are visible. Clusters containing up to eight carrier gas particles are readily observed.

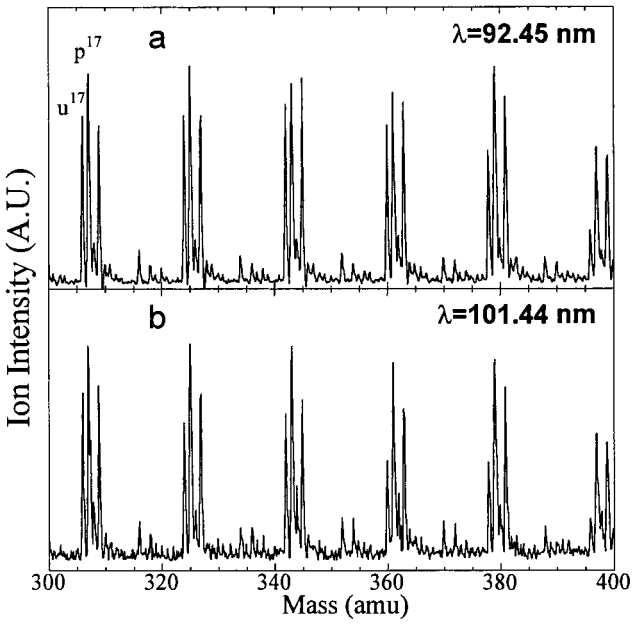

Figure 6. (a) Mass spectrum recorded using a strong H_2O/Ar expansion. Protonated and unprotonated water clusters as well as daughter ions are observed. Ionization is performed with 92.45 nm radiation. (b) Mass spectrum obtained using similar conditions as used in (a). Ionization is now performed with 101.44 nm radiation. The spectra are very similar, and the minor differences can be explained by slight differences in expansion conditions.

only be formed when expansion conditions are strong enough to produce neutral water clusters with adsorbed Ar. To more fully explore this phenomenon, we have measured photoionization mass spectra for a number of carrier gases, M = Kr, O_2, N_2, CO_2, and CO. All of these carrier gases exhibited qualitatively similar behavior to Ar. In all cases we are able to observe the u^n family always in coincidence with u^nM_m families. Figure 5 gives a particularly striking example for M = CO, where unprotonated water clusters containing up to eight CO molecules can be observed as parent ions. For spectra produced using CO as a carrier gas, the sum of unprotonated and binary water clusters ($u^n + u^n(CO)_m$) is responsible for approximately 80% of the observed cluster signal. This value is only weakly dependent on *n*. Interestingly, when He and Ne were used as carrier gases, neither u^n, u^nHe_m, nor u^nNe_m could be observed under any expansion conditions. This is consistent with the idea that mixed neutral clusters must first form in the molecular beam expansion before unprotonated water clusters can be observed. It is reasonable that mixed H_2O/Ne and H_2O/He clusters would be the most difficult to form since the binding energy of these two noble gases to water is substantially lower than all of the other carrier gases used in this work.

Conceptually, there are only two ways that suppression of fragmentation may occur: *soft ionization* or *active parent ion cooling*. Small unprotonated water clusters ($n = 2-5$) have been reported for the first time by Shinohara et al.[2] As in this work, unprotonated ions were only found under strong expansion conditions using Ar as a carrier gas. For these small clusters it was suggested that direct photoexcitation to the $H_3O^+ \cdot OH(H_2O)_{n-2}$ structure was made possible when Ar was adsorbed to the neutral cluster. The authors argued that the Franck−Condon factor (FCF) for direct ionization to an unprotonated water cluster, normally extremely small due to contraction of the O−O bond upon ionization, is enlarged due to the presence of Ar atoms in mixed H_2O/Ar clusters, which supposedly prevented the contraction of the O−O bond on ionization. Assuming that were true, the FCF for ionization might only depend on the wave functions of the transferred proton in the neutral and ion state, which, being a light atom, might give rise to a large FCF. If this picture were true, this would suggest that the presence of adsorbed carrier gas actually allows a novel form of soft ionization, suppressing fragmentation.

Such a mechanism is, however, inconsistent with the heavy water results shown above. We noted no substantial quantitative differences between H_2O and D_2O clusters regarding their tendency to form unprotonated water cluster ions. If the formation of unprotonated water clusters was determined by the overlap integral of the transferred protons (or deuterons) wave functions in the neutral and ion state, a large isotope effect would be expected. Arguably, there should be no u^n ions for heavy water. This hypothesis furthermore suggests that there is something special about the Ar $(H_2O)_n$ interaction that stabilizes the ion structure to make it look more similar to the neutral structure. It would be a remarkable coincidence if this behavior were similar for all of the carrier gases that we have examined. Furthermore, such a "soft ionization" mechanism is only possible for small clusters (if at all). In large clusters the largest contribution to the parent ion internal energy does not come from the proton transfer reaction but from the solvent reorganization. The FCF's for all of the solvent coordinates must also be taken into consideration, and therefore, this model clearly predicts that the probability for forming u^n decreases with *n*, directly opposite to what is observed in this work.

Another way to gain insight into the ionization process is to examine the dependence on the photoionization wavelength. One might, for example, expect that if a "soft ionization" mechanism were important in the formation of the u^n family, the ratio of u^n to p^n might change dramatically with the wavelength of the ionizing radiation. In all of the results reported so far, the energy of the ionizing photons (13.4 eV) is larger than the ionization potential (IP) of the water monomer (12.61 eV). The vertical IP of water clusters is lower than that of the water monomer and is decreasing with cluster size and stabilizes around 11.0 eV for clusters containing more than eight water monomers.[5] Figure 6 shows mass spectra as recorded under conditions where both protonated and unprotonated clusters ions are formed. Figure 6a shows the spectrum measured using 92.45 nm (13.4 eV) photons, while Figure 6b shows the spectrum obtained using

101.44 nm (12.2 eV) light for ionization. The 101.44 nm radiation is produced using the second harmonic of the PDL-1 running on Rhodamine 640 dye and using Ar as the tripling gas. Using the integrated peak intensities to calculate the fraction of unprotonated to protonated ions as well as the total fraction of carrier gas containing clusters, no meaningful difference (outside of the experimental error) can be found. The small apparent differences in Figure 6 can be explained by a minor change in expansion conditions. Because the ratio between protonated and unprotonated cluster signal depends critically on timing between gas pulse and laser, a slight change in the expansion conditions results in a relatively large change of this ratio. On the basis of all of the considerations presented above, we must conclude that a soft ionization mechanism based on enhanced FCF's resulting from carrier gas adsorption is highly unlikely, at least for the large clusters observed in this work.

The most likely explanation for the observation of the unprotonated clusters is rapid evaporative cooling. Upon ionization of mixed H_2O/M water clusters, proton transfer and solvent reorganization occur. This is expected to initially deposit between 2 and 3 eV of internal energy into the parent ion. In contrast to pure water clusters, this excess energy can be rapidly removed by the evaporation of the carrier gas. Once the energy in the cluster ion is low enough (possibly even freezing the water cluster), the mobility of the OH radical in the cluster is sufficiently reduced that the OH radical is trapped in the cluster, leading to the formation of the "unprotonated" clusters. The model is also consistent with the observation of u^nM_m ions (carrier gas containing clusters) which have been sufficiently cooled after only a fraction of the carrier gas molecules have been evaporated. The proposed mechanism relies on the assumption that the carrier gas particles evaporate much more quickly from the cluster than do water molecules, thus cooling the cluster before the loss of OH can occur. Such behavior can actually be observed under favorable conditions in a PSD experiment. Figure 7 shows the TOF spectrum using the mass gate to select a small number of parent ions observed under strong expansion conditions with N_2 carrier gas. The region of the mass spectrum near u^{14} and p^{14} is shown. The peaks to the right of the dashed vertical line are mainly due to parent ions selected by the mass gate. The peaks left of this line are mainly due to daughter ions, although the very small peaks around 41.1 μs result from "leaking" of carrier gas containing mixed cluster parent ions through the mass gate.

Assignment of parent ions of interest is also shown in the figure. The three largest daughter ion peaks, left of the dashed line, are also labeled in the figure. They result from the following PSD channels: (1) $p^{14} \rightarrow p^{13} + H_2O$ in combination with $u^{13}N_2 \rightarrow u^{13} + N_2$, (2) $u^{10}(N_2)_3 \rightarrow u^{10}(N_2)_2 + N_2$, and (3) $u^7(N_2)_5 \rightarrow u^7(N_2)_4 + N_2$. One should also note that, as described above, it is highly likely that at least some of the peak labeled $p^{14} \rightarrow p^{13} + H_2O$ is also made up of $u^{14} \rightarrow p^{13} + OH$, which cannot be resolved for beams of light water clusters. The fraction of mixed parent ions that lose a nitrogen molecule for all of these species is around 20%. Note that evaporation of water monomers from u,[14] $u^{13}(N_2)$, $u^{10}(N_2)_3$, and $u^7(N_2)_5$, indicated by the dashed arrows labeled "a−d", respectively, is not observed. (Loss of water from u^{14}, arrow a, is below 5%, assuming the small peak observed is completely due to this effect and not due to "leaking" of another parent ion). A similar observation has been reported for $(H_2O)_6Ar_n$ anions.[23] The data of Figure 7 give direct evidence that the rate of evaporation of

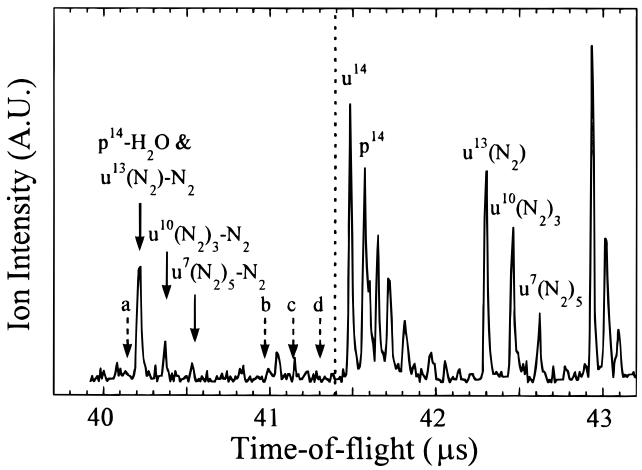

Figure 7. TOF spectrum as recorded when the mass gate is applied to only select the mass region between 14-mer and 15-mer. The spectrum is recorded for a strong H_2O/N_2 expansion. Peaks right of the vertical dashed line are mainly due to parent ions, and the peaks left of this line are dominantly due to daughter ions. The relevant parent ion peaks are indicated in the figure. The largest daughter ion peak is due to metastable decay of the 14-mer, as well as due to loss of N_2 from the binary cluster containing only one carrier gas particle. The smaller daughter ion peaks are assigned in the figure as well. The dashed vertical arrows show the position where peaks due to loss of a single water monomer from the unprotonated cluster, and the binary clusters containing 1, 3, and 5 carrier gas particles, respectively, are expected to appear. The data shows that N_2 evaporation from the unprotonated clusters is much more rapid than H_2O evaporation.

adsorbed carrier gas particles can be much more rapid than that of water from binary cluster ions.

Consideration of simple kinetic principles also predicts that the rate of inert gas evaporation will be higher than that for evaporation of water, regardless of the energy of the system. Recall that the Arrhenius relation, $k(T) = A \exp(-E_a/RT)$, is composed of a preexponential (A) factor, which is related to the entropy of the transition state, and an activation energy (E_a), which is related to the energy of the transition state. Comparing evaporation of Ar vs water, we expect E_a(Ar) to be less than $E_a(H_2O)$ on energetic grounds. More importantly, for the first stages of parent ion fragmentation, the entropy of the transition state for evaporation of Ar is expected to be much higher than that for water (A(Ar) $\gg$ $A(H_2O)$). This results from the fact that water evaporation requires a substantial reorganization of the hydrogen-bonded network in the cluster, whereas Ar evaporation does not. Both of these considerations lead one to conclude that evaporation of inert (i.e., non-hydrogen-bonded) gas will be much more rapid than evaporation of water, both at low and at high energy.

Further evidence for the importance of evaporative cooling by Ar has recently been suggested in connection with cluster formation in a pickup cell. In those experiments, $SF_6(CO_2)_n$ clusters formed by pickup of SF_6 on CO_2 clusters was only observed when mixed Ar/CO_2 clusters were used as a precursor. It is likely that the evaporation of Ar atoms from the mixed clusters serves to dissipate the collision energy associated with the "pickup" of the SF_6 molecule.[24]

Post Source Decay Studies: Rapid Evaporative Cooling of Protonated Cluster Ions. In this section we continue to present more evidence for the importance of rapid evaporative cooling. So far, we have restricted our arguments to the role of rapid evaporative cooling on the u^n family of parent ions. We have shown strong evidence that when neutral water clusters are formed with carrier gas adsorbed on them, the energy

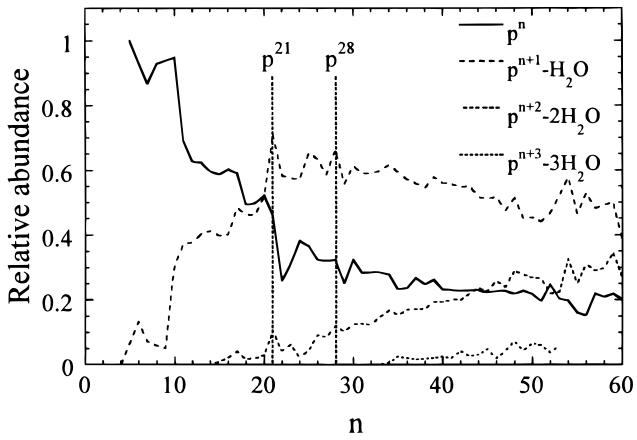

Figure 8. Relative abundance of parent and daughter ions of the protonated water cluster family under mild beam conditions as a function of cluster size. The horizontal axis is associated with the cluster size of the product ion, and not with the size of the parent ion. For the parent ions the relative abundance is equal to the survival probability at the time that the first grid of the reflectron is reached. For the daughter ions it corresponds to the fraction of the parents ions that decays to provide the specific daughter ion. Effects due to "magic" number protonated clusters ions (cluster size indicated by the vertical dashed line) are discussed in the text.

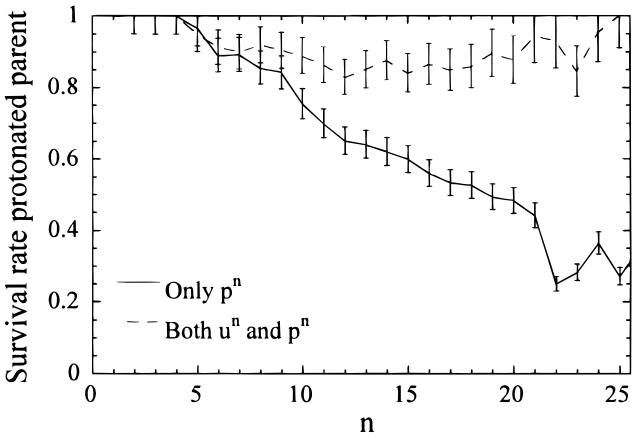

Figure 9. Survival probability of protonated D_2O clusters at the moment that they reach the first grid of the reflectron as a function of cluster size for conditions without (solid line) and with (dashed line) unprotonated clusters present. The survival rate for the latter condition is observed to be much higher, indicating that the protonated clusters produced under these conditions are much colder and also result from mixed clusters that have undergone evaporative cooling.

deposited upon ionization can be efficiently carried away. If this is true, one would also expect that there must be a distribution of neutrals, some containing many carrier gas atoms and some containing only a few. Consequently, it would not be surprising if those neutrals containing only a few carrier gas atoms were not completely successful in suppressing loss of OH. Yet even in this case, where the cooling of the parent ion is insufficient to suppress the fastest fragmentation channel, the amount of energy that is removed by the evaporative cooling process should appear as reduced rates in PSD. Indeed, it would be difficult to understand how the fragmentation of the u^n parents could be strongly affected by rapid evaporative cooling while the fragmentation of the p^n parents were unaffected. We have therefore carried out a systematic investigation of the PSD of the protonated water cluster ions under conditions where we can exclude mixed cluster ions and compared that to conditions where we know mixed clusters are present. The results are quite revealing.

Figure 8 shows the fraction of protonated parent (p^n) and daughter ions ($p^{n-1} + H_2O$, $p^{n-2} + 2H_2O$, and $p^{n-3} + 3H_2O$) formed in PSD under mild expansion conditions where there is no evidence of mixed water clusters. For clarity, the error bars (typically 10% of the calculated value) are not indicated in the figure. The results are derived simply by integrating assigned parent and daughter peaks. For this analysis we neglect the minor contributions due to ISD. The value "*n*" on the horizontal axis refers to the final product ion formed in PSD and not to the parent ion. Consequently, the total fraction for each value of *n* does not sum to unity.

The survival probability of the protonated parent ions measured here is in good agreement with earlier data recorded by Shi et al.,[8] from which the binding energy as a function of cluster size is obtained by applying the model proposed by Klots.[25] Although the decay rate due to loss of the first water monomer is almost identical to the value that can be extracted from our experiments, they do not observe loss of more than a single water monomer, a difference that may be due to their use of a different ionization scheme. In this work it is obvious that the survival probability for p^n drops precipitously with *n* until reaching a value of about 0.2 near $n = 50$. Evidence for more stable "magic" number clusters, particularly p^{21}, but also p^{28}, can again be observed.

To obtain similar PSD survival probabilities for the p^n family under conditions where mixed clusters are present and the u^n family is also present in the mass spectrum, it is necessary to again resort to heavy water beams. Only then can the decay processes $u^n \rightarrow p^{n-1} + OD$ and $p^n \rightarrow p^{n-1} + D_2O$ be resolved in time, as mentioned above.

The survival probabilities for p^n under different beam conditions are presented in Figure 9. The solid line is for heavy water beams under conditions where no mixed clusters are present and only the p^n family is present in the mass spectrum. As for light water (see Figure 8), there is a precipitous drop in the survival probability as *n* increases; ion decay is dominated by $p^n \rightarrow p^{n-1} + D_2O$. The dashed line shows the survival probability of p^n (i.e., due to suppression of $p^n \rightarrow p^{n-1} + D_2O$) under beam conditions where mixed clusters are known to be present. One can clearly see that, within our experimental error, the evaporation of water from the protonated cluster ions has been essentially eliminated. This is further evidence that rapid evaporative cooling is the proper explanation of the observations presented in this paper.

Conclusions

We have presented an extensive study of the decay dynamics of pure and mixed water cluster ions produced by single-photon ionization of neutral clusters. We observe that the mass spectrum is strongly dependent on the expansion conditions. When water clusters with carrier gas adsorbed to them are photoionized, "unprotonated" water clusters are observed, which is a manifestation of the dramatically reduced role of parent ion fragmentation under these conditions. Analysis of the post source decay of the unprotonated water clusters using beams of heavy water reveals that the structure is best described as a solvated H_3O^+ molecule with an OH radical caged somewhere in the cluster: $H_3O^+(H_2O)_{n-2}\cdot OH$. The mechanism for the formation of these "unprotonated" water cluster ions is *active parent ion cooling* resulting from rapid evaporation of carrier gas atoms or molecules that have been preadsorbed onto the water clusters. The influence of rapid evaporative cooling is also observed in the suppression of fragmentation of the protonated water cluster ions. Direct observation of the rate of

evaporation of N_2 vs H_2O was possible in a post source decay experiment, explicitly showing that the evaporation of the carrier gas can be the dominant cooling mechanism.

In recent years molecular beam and laser desorption techniques have rapidly advanced our ability to put very large involatile polymeric compounds into the gas phase. Mass spectrometry of such compounds (for example, using MALDI) has proven to be enormously beneficial, for example, in analysis of polypeptide mixtures. Still one of the biggest hindrances to the application of advanced mass spectrometric methods to biopolymers and other technologically important polymeric compounds is our inability to control the fragmentation of the parent ions. In such cases, it is quite difficult to obtain the initial polymer mixture constituency from the mass spectrum. The possibility of applying the lessons we have learned from the study of one of the most fragile polymeric compounds existing in nature, i.e., $(H_2O)_n$, to technologically more significant polymeric compounds is very intriguing. Such studies are planned for the very near future.

Acknowledgment. This work was made possible by a grant from the National Science Foundation (9633002).

References and Notes

(1) Ng, C. Y.; Trevor, D. J.; Tiedemann, P. W.; Ceyer, S. T.; Kronebusch, P. L.; Mahan, B. H.; Lee, Y. T. *J. Chem. Phys.* **1977**, *67*, 4235.

(2) Shinohara, H.; Nishis, N.; Washida, N. *J. Chem. Phys.* **1986**, *84*, 5561.

(3) Fröchtenicht, R.; Kaloudis, M.; Koch, M.; Huisken, F. *J. Chem. Phys.* **1996**, *105*, 6128.

(4) Levin, R. D.; Lias, S. G. *Ionization Potential and Appearance Potential Measurements 1971*; U.S. GPO: Washington, DC, 1982.

(5) Tomoda, S.; Kimura, K. *Chem. Phys. Lett.* **1983**, *102*, 560.

(6) Novakovskaya, Y. V.; Stepanov, N. F. *Int. J. Quantum Chem.* **1997**, *61*, 981.

(7) Kobayashi, C.; Iwahashi, K.; Saito, D.; Ohmine, I. *J. Chem. Phys.* **1996**, *105*, 6358.

(8) Shi, Z.; Ford, J. V.; Wei, S.; Castleman, A. W., Jr. *J. Chem. Phys.* **1993**, *99*, 8009.

(9) Gough, T. E.; Mengel, M.; Rowntree, P. A.; Scoles, G. *J. Chem. Phys.* **1985**, *83*, 4958.

(10) Scheideman, A.; Schilling, B.; Toennies, J. P. *J. Phys. Chem.* **1993**, *97*, 2128.

(11) Ehbrecht, M.; Stemmler, M.; Huisken, F. *Int. J. Mass Spectrom. Ion Processes* **1993**, *123*, R1.

(12) Dagan, S.; Amirav, A. *J. Am. Soc. Mass Spectrom.* **1996**, *7*, 550.

(13) Mamyrin, B. A.; Karataev, V. I.; Shmikk, D. V.; Zauglin, V. A. *Sov. Phys. JETP* **1973**, *37*, 45.

(14) Page, R. H.; Larkin, R. J.; Kung, A. H.; Shen, Y. R.; Lee, Y. T. *Rev. Sci. Instrum.* **1987**, *58*, 1616.

(15) Tonkyn, R. G.; White, M. G. *Rev. Sci. Instrum.* **1989**, *60*, 1245.

(16) Wiley, W. C.; McLaren, I. H. *Rev. Sci. Instrum.* **1955**, *26*, 1150.

(17) Wei, S.; Castleman, A. W., Jr. *Int. J. Mass Spectrom. Ion Processes* **1994**, *131*, 233.

(18) Magnera, F. T.; David, D. E.; Michl, J. *Chem. Phys. Lett.* **1991**, *182*, 363.

(19) Kühlewind, H.; Kiermeier, A.; Neusser, H. J. *J. Chem. Phys.* **1986**, *85*, 4427.

(20) Searcy, J. Q.; Fenn, J. B. *J. Chem. Phys.* **1974**, *61*, 5282.

(21) Echt, O.; Kresile, D.; Knapp, M.; Recknagel, E. *Chem. Phys. Lett.* **1984**, *108*, 401.

(22) Nagashima, U.; Shinohara, H.; Nishi, N.; Tanaka, H. *J. Chem. Phys.* **1986**, *84*, 209.

(23) Ayotte, P.; Bailey, C. G.; Kim, J.; Johnson, M. A. *J. Chem. Phys.* **1998**, *108*, 444.

(24) Jones, A. B.; Woodward, C. A.; Winkel, J. F.; Stace, A. J. *Int. J. Mass Spectrom. Ion Processes* **1994**, *133*, 83.

(25) Klots, C. E. *J. Chem. Phys.* **1985**, *83*, 5854−5860; *Z. Phys. D* **1991**, *21*, 335.